Polypropylene-substrate-based SRR- and CSRR-metasurfaces for submillimeter waves

M. Aznabet[1], M. Navarro-Cía[1], S. A. Kuznetsov[2], A. V. Gelfand[3], N. I. Fedorinina[3], Yu. G. Goncharov[4], M. Beruete[1], O. El Mrabet[1], and M. Sorolla[1]

[1]*Millimeter and Terahertz Waves Laboratory, Universidad Pública de Navarra, Campus Arrosadía, 31006 Pamplona, Spain*
[2]*Budker Institute of Nuclear Physics SB RAS, Lavrentiev Ave. 11, 630090 Novosibirsk, Russia and Novosibirsk State University, Pirogova Str. 2, 630090 Novosibirsk, Russia*
[3]*Institute of Semiconductor Physics SB RAS, Novosibirsk Branch "TDIAM", Nikolaeva Str. 8, 630090 Novosibirsk, Russia.*
[4]*General Physics Institute RAS, Vavilov Str. 38, 119991 Moscow, Russia*
**Corresponding author: mario@unavarra.es*

Abstract: In this paper it is presented the fabrication of low loss millimeter wave metamaterials based on patterning on polypropylene substrates by conventional contact photolitography. We study numerically and experimentally the transmission and reflection properties of two dimensional arrays of split ring resonators (SRRs), or metasurfaces, and their complementary structure (CSRRs) for co- and cross-polarization excitations up to submillimeter frequencies under normal incidence conditions. The obtained results suggest the possibility of scaling them at terahertz frequencies based on this substrate where other lossy substrates degrade the resonators quality. Left-handed metamaterials derived from these SRRs and CSRRs metasurfaces could be feasible.

OCIS codes: (160.3918) Metamaterials; (350.3618) Left-handed materials

References and Links

1. V.G. Veselago, "The Electrodynamics of Substances with Simultaneously Negative Values of ε and μ," Sov. Phys. Usp. **10**, 509-514 (1968).
2. R. Marqués, F. Martin, and M. Sorolla, *Metamaterials with Negative Parameter: Theory, Design, and Microwave Applications* (New York: Wiley, 2008).
3. D. R. Smith, W. J. Padilla, D. C. Vier, S. C. Nemat-Nasser, and S. Schultz, "Composite medium with simultaneously negative permeability and permittivity," Phys. Rev. Lett. **84**, 4184-4187 (2000).
4. J. B. Pendry, A. J. Holden, W. J. Stewart, and I. Young, " Extremely low frequency plasmons in metallic mesostrucutres," Phys. Rev. Lett. **76**, 4773-4776 (1996).
5. J. B. Pendry, A. J. Holden, D. J. Robbins, and W. J. Stewart, "Magnetism from conductors and enhanced nonlinear phenomena," IEEE Trans. Microwave Theory Tech. **47**, 2075-2084 (1999).
6. F. Falcone, T. Lopetegi, M.A.G. Laso, J. D. Baena, J. Bonache, M. Beruete, R. Marqués, F. Martín, and M. Sorolla, "Babinet principle applied to metasurface and metamaterial design," Phys. Rev. Lett. **93**, 197401-1-4 (2004).
7. R. Marqués, F. Medina, and R.R. El-Idrissi, "Role of Bianisotropy in Negative Permeability and Left-Handed Metamaterials," Phys. Rev. *B* **65**, 144440 1-6 (2002).
8. M. Beruete, M. Sorolla, R. Marqués, J. D. Baena, and M. J. Freire, "Resonance and Cross-Polarization Effects in Conventional and Complementary Split Ring Resonator Periodic Screens," Electromagnetics **26**, 247-260 (2006).
9. T. J. Yen,W. J. Padilla, N. Fang, D. C. Vier, D. R. Smith, J. B. Pendry, D. N. Basov, and X. Zhang, "Terahertz Magnetic Response from Artificial Materials," Science **303**, 1494-1496 (2004).
10. W. J. Padilla, M. T. Aronsson, C. Highstrete, Mark Lee, A. J. Taylor, and R. D. Averitt, "Electrically resonant terahertz metamaterials: Theoretical and experimental investigations," Phys. Rev. B **75**, 041102-1-4 (2007)
11. H. T. Chen, J. F. O'Hara, A. J. Taylor, R. D. Averitt, C. Highstrete, M. Lee, and W. J. Padilla, "Complementary planar terahertz metamaterials," Opt. Express **15**, 1084-1095 (2007).
12. Y. Yuan, C. Bingham, T. Tyler, S. Palit, T. H. Hand, W. J. Padilla, D. R. Smith, N. M. Jokerst, and S. A. Cummer, "Dual-band planar electric metamaterial in the terahertz regime," Opt. Express **16**, 9746-9752 (2008).

#100467 - $15.00 USD Received 22 Aug 2008; revised 8 Oct 2008; accepted 10 Oct 2008; published 23 Oct 2008

13. N. Liu, H. Guo, L. Fu, S. Kaiser, H. Schweizer, and H. Giessen, "Three-dimensional photonic metamaterials at optical frequencies," Nature Materials, **7**, 31-37 (2007).
14. M. Beruete, M. J. Freire, R. Marqués, F. Falcone, and J. D. Baena, "Electroinductive waves in chains of complementary metamaterial elements," Appl. Phys. Lett. **88,** 083503-1-3 (2006).
15. M. Beruete, M. Sorolla, and I. Campillo, "Left-handed extraordinary optical transmission through a photonic crystal of subwavelength hole arrays," Opt. Express **14**, 5445-5455 (2006).
16. J. García-García, F. Martín, J. D. Baena, R. Marques, and L. Jelinek, "On the resonances and polarizabilities of split ring resonators," J. Appl. Phys. **98**, 033103-1-9 (2005).
17. C. Dahl, P. Goy, and J. P. Kotthaus, "Magneto-optical Millimeter-Wave Spectroscopy" and G. V. Kozlov and V. V. Volkov. "Coherent Source Submillimeter Wave Spectroscopy," in *Millimeter and Submillimeter Wave Spectroscopy of Solids (Topics in Applied Physics, Vol. 74)*, (Springer-Verlag Berlin Heidelberg, Ed.: G. Gruener, 1998) pp. 51-109.

1. Introduction

The concept of left-handed metamaterials (LHM), which require simultaneous negative permittivity ε and negative permeability μ, was studied theoretically for the first time by Veselago [1] decades ago. He found that Maxwell's equations lead to a special case when both electric permittivity and magnetic permeability of the matter in which a monochromatic plane wave is propagated are negative. This solution corresponds to a material with a negative refractive index. This property not found in natural materials, opens up the gate to a field of novel, exotic phenomena such as inverse Snell's law in the interface between a standard and a left-handed medium, near-field amplification, perfect lensing, and reversed of Doppler and Cerenkov effects [2]. It was Smith et al. [3] who confirmed experimentally the inversion of Snell's law at microwave frequencies by combining a thin wire medium [4] and split ring resonators (SRRs) [5] in a composite structure, enabling the electric permittivity and magnetic permeability to be simultaneously negative within a certain frequency bandwidth.

So far, SRRs are the most common particle to realize negative permeability for synthesizing LHMs. Recently, the dual structure of the split ring resonator, called complementary split ring resonator (CSRR), has been studied as an alternative to SRR for some applications [6]. The main characteristic that makes SRRs/CSRRs very interesting for the design of artificial media is that their first resonance is quasi-static [6,7], so that SRRs/CSRRs electrical size at such resonance is small enough to allow for a continuous media modelling of the composite. Moreover, their bianisotropy property [7] allows for the design of frequency selective surfaces or metasurfaces based on these particles [8].

Realization of low-loss LHMs synthesized using this kind of particles at higher frequencies would open a way for many applications. In this sense, metasurfaces design and dual band operation has been demonstrated at terahertz wavelengths [9-12] and at optical ones where even a left-handed metamaterial by stacking U-shaped particles has been shown [13].

In the present work, we study numerically and experimentally up to the submillimeter waves band (0.55 THz) the transmission and the reflection properties of not only an array of SRRs, but also their complementary structure etched on a polypropylene (PP) substrate. The characterization is done with two orthogonal polarizations under normal incidence. Therefore, we will focus on the fabrication technique and the behavior of single metasurfaces. Note that our approach differs from that of [11] in the different nature of our fabrication method (patterning Al-layers on low-losses polypropylene substrates by conventional contact photolithography) instead of patterning on semi-insulating gallium arsenide (SI-GaAs) substrates as in [11]. Moreover, we have used squared arrays of classical Pendry's SRR [5] and CSRR [6] instead of the planar electric split ring resonator (eSRR) and its Babinet complementary used in [11].

In a subsequent work we will study the features that appear when SRR/CSRR metasurfaces are stacked and, in particular, we will show that stacked CSRR metasurfaces exhibit LH propagation thanks to the excitation of electroinductive waves [2,14], with a mechanism similar to stacked subwavelength hole arrays [15].

#100467 - $15.00 USD Received 22 Aug 2008; revised 8 Oct 2008; accepted 10 Oct 2008; published 23 Oct 2008

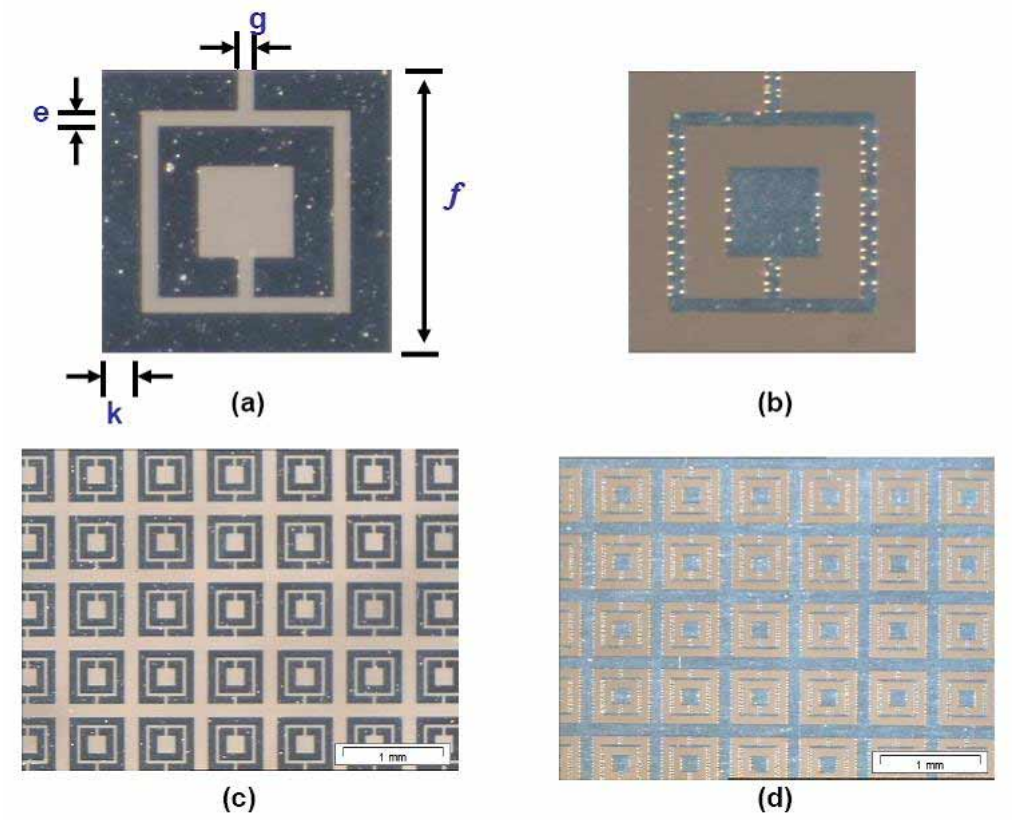

Fig. 1. Geometry of (a) a square CSRR and (b) a square SRR. (c) Microscopic image of a square CSRR array with the following dimension: e = 30 μm, g = 30 μm, k = 80 μm, f = 0.56 mm, and lattice constant is 0.7 mm. (d) Microscopic image of a square SRR array.

2. Design of SRRs and CSRRs metasurfaces.

The unit cell geometries are shown in Fig. 1(a) and Fig. 1(b) respectively. The SRR has an outer dimension of f = 0.56 mm, a lattice parameter of 0.7 mm (a quarter of free space wavelength, λ/4, at the first resonant frequency of the SRR), line width of k = 80 μm, and a gap of e = 30 μm. If we replace the metallic parts of SRR by apertures and apertures by metallic parts, a CSRR is obtained as shown in Fig. 1(b). These dimensions have been selected to place the quasi-static resonance at the lower portion of our experimental bandwith (60 GHz; V-band) and, therefore, to keep the remaining measurement bandwith to observe the higher-order resonances.

Both metasurfaces are designed as square planar arrays on PP substrate of 20 μm thickness (see section 3 for details on fabrication). The choice of PP is due to its low dispersion and small dielectric losses (tan δ = 0.0005) within a very wide frequency range from microwave to infrared frequencies. It is also worthwhile to mention that PP could be considered a good polymer for metamaterial applications owing to its high mechanical fastness, chemical resistance, better adhesion and higher melting temperatures in comparison with polyethylene, as well as commercial availability.

The use of this polymer to minimize losses may open the possibility of scaling left-handed metamaterials deriving from split ring resonators and their complementary structures to terahertz frequencies.

#100467 - $15.00 USD Received 22 Aug 2008; revised 8 Oct 2008; accepted 10 Oct 2008; published 23 Oct 2008

3. Technology of prototype fabrication.

The process of metasurface fabrication begins with vacuum thermal deposition of the aluminum layer 0.5 μm thick onto the surface of a PP film which is stretched tightly over the bearing glass wafer with outer sizes 102x102 mm. Commercial PP-films with specially processed surface for improving adhesion of Al to PP were used. For creating a metasurface micro-pattern in the deposited Al-layer we employed a conventional technology of contact photolithography widely applied in semiconductor ("Si-line") industry. The technology includes the following stages:

1. Spin coating process based deposition of a 0.6μm-thick positive photoresist film onto the surface of the Al-layer with following air drying (20 min) and thermal treatment in a thermostat at 90^0C (20–25 min) for fixing of the photoresist.
2. Photoresist exposure by monochromatic UV-radiation (λ=365 nm) via the "positive" photomask set in contact with the photoresist layer for creating a latent resistive image of the desired output metastructure micro-pattern which replicates the micro-pattern of the photomask. The photomask micro-pattern is created in advance by electron- or laser-beam lithography in a chromic- or ferric-oxide-film deposited onto a photomask quartz wafer. Typically we increase the width of photomask opaque areas by 1μm with respect to the output micro-pattern values as at the stage 5 of chemical etching of the Al-layer its edges sink at 0.5μm.
3. Photoresist development in the solution of *KOH* for removing irradiated (transparent) areas of photoresist. The topological dimensions of the developed resistive mask are checked by optical microscopy at this intermediate stage.
4. Compressed air drying and thermal treatment of the developed photoresist in a thermostat at 120^0C (30 min) for hardening the photoresist required for its withstanding during the next stage.
5. Chemical etching of the 0.5μm-thick-Al-layer through the hardened resistive mask using inorganic solvents.
6. Chemical removal of the hardened photoresistive material in an organic solvent, and the final microscopic control of dimensions for the finished output Al-metastructure.
7. After completing the photolithography procedure a thin-film metastructure is separated from the glass wafer and is tightly ("drum-like") tightened onto a ring-shaped metal holder with clear aperture diameter 50 mm.

We revealed that standard commercial PP-films exhibit surface microdefects which result in flaking away the Al-coating in the points of defects during the fabrication process. This effect can be seen in Fig. 1. Improving adhesion of Al by deposition of a thin auxiliary intermediate layer of Ti or Cr partly solves the problem of flaking, however ultimate minimization of surface defects can be realized by improving original quality of employed PP-films.

4. Simulation and experimental results.

In the simulations made by CST Microwave Studio™, a commercial simulator based on Finite Integration Time Domain Method (FITD), the free-space set up is simulated with a unit cell surrounded by mutually orthogonal electric and magnetic walls as boundary conditions on the transverse directions and open boundary conditions along the wave propagation. Both SRR and CSRR metasurfaces have been simulated with co- and cross-polar excitations (Field orientation in each case is explicitly shown in the insets of Figs. 2 and 3 of the present manuscript. See Ref. 8 for a detailed description). Transmission as well as reflection results are shown in Figs. 2 and 3 with a bandwidth from 40 to 525 GHz in transmission and from 40 to 170 GHz in the reflection case. These bandwidths are dissimilar in order to fit with the technological constraints imposed by the measurement.

The frequency responses of both structures were measured in two steps, one by using an AB Millimetre™ Quasioptical Vector Network Analyzer equipment in the frequency range of 40 to 260 GHz and, second, from 260 up to 525 GHz by means of a submillimeter wave

#100467 - $15.00 USD Received 22 Aug 2008; revised 8 Oct 2008; accepted 10 Oct 2008; published 23 Oct 2008

BWO-based spectrometer. Therefore our measurement covers the wavelength range from 0.57 mm up to 7.50 mm). Details of the instrumentation can be found in [17]. The measurements procedure is as follows: a horizontally or vertically polarized gaussian beam is generated by a transmitting corrugated horn antenna. This beam propagates up to a focusing pair of elliptical mirrors or polyethylene lenses designed to obtain an undistorted beam having its beam waist in the half of the distance, where the sample is located. Finally, power distribution at the output is received with another corrugated horn antenna located far away from the transmitted horn antenna. The calibration is made by simply removing the structure under study and maintaining the rest of the whole set-up.

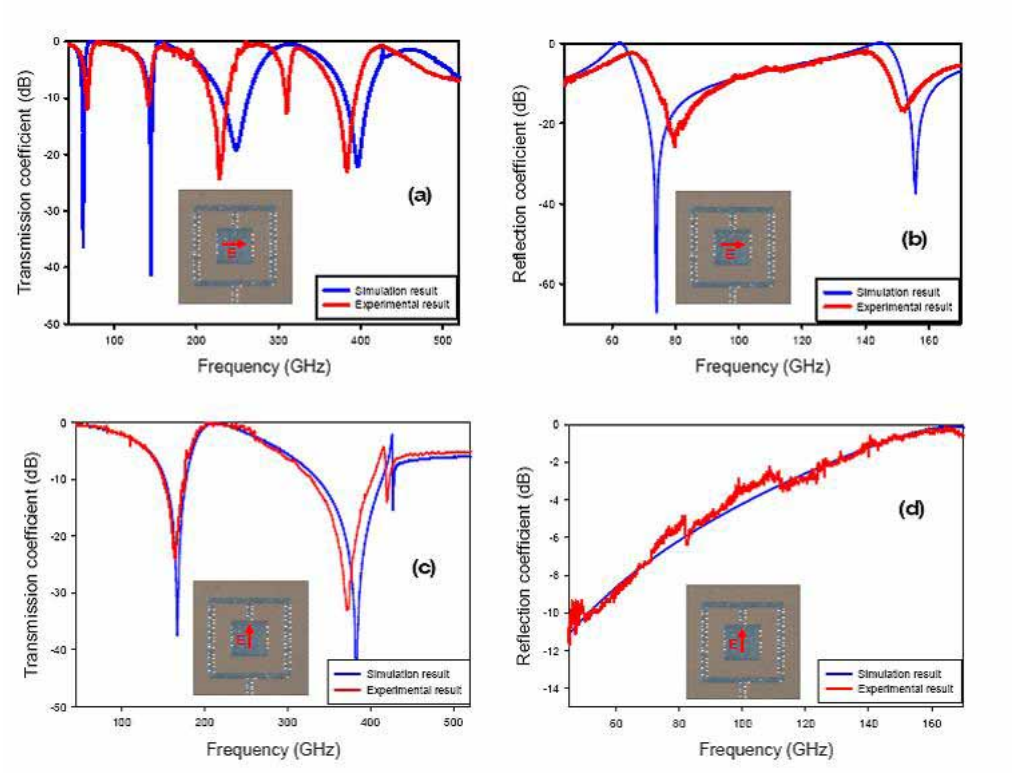

Fig. 2. Simulated (blue) and measured (red) results of fabricated SRRs array. Co-polar transmission (a) and reflection (b) coefficients. Cross-polar transmission (c) and reflection (d) coefficients.

Throughout the frequency response for the SRR case (see Fig. 2), five experimental transmission dips are observed for the co-polar case whereas in the simulation only four dips are obtained. In the cross-polar case two dips appear both in simulation and experiment. More specifically, the first co-polar SRRs resonance is placed at 66.5 GHz which is a quasistatic resonance as it is well known [7]. The following upper order resonances appear at 145 GHz, 230 GHz (250 GHz in the simulation), 310 GHz (does not appear in simulation), 380 GHz (400 GHz in simulation). The cross-polar dips appear at 170 GHz and 370 GHz and practically coincide in simulation and experiment.

On the other hand, for CSRR case (see Fig. 3), we obtain a nearly complementary response [6] of SRR case, as it was expected due to the presence of the PP film. From the measured frequency response for the CSRRs, six transmission distinct maxima appear for the co-polar case, while the simulation predicts five. In the cross-polar configuration there are two peaks in both cases. In detail, the first co-polar CSRRs resonance is placed at 70 GHz. The following upper order resonances appear at 145 GHz, 230 GHz, 310 GHz, 380 GHz and a final peak at 510 GHz. In the simulation the peak at 310 GHz is lost and the remainder peaks appear at the

#100467 - $15.00 USD Received 22 Aug 2008; revised 8 Oct 2008; accepted 10 Oct 2008; published 23 Oct 2008

same location as in the experiment. The cross-polar the peaks appear at 160 GHz and 350 GHz in both cases.

It is noticeable the very low losses level measured for both SRR and CSRR metasurfaces which makes this substrate a potential candidate for terahertz and optical metamaterials.

In addition to the previously presented transmission properties, we also show the measured reflection coefficient for both structures exhibiting only the first and the second resonances and with respect to co- and cross-polarizations as displayed in panels (b) and (d) of Figs. 2 and 3, respectively. It is important to notice that due to hardware limitations of our experimental facilities this reflection measurement is performed up to 170 GHz.

Here, the first co-polar SRRs resonance peak is placed at 66 GHz. The following upper order resonance appears at 140 GHz. For the cross-polar, the peak appears at 166 GHz. Again, simulation and measurement agree.

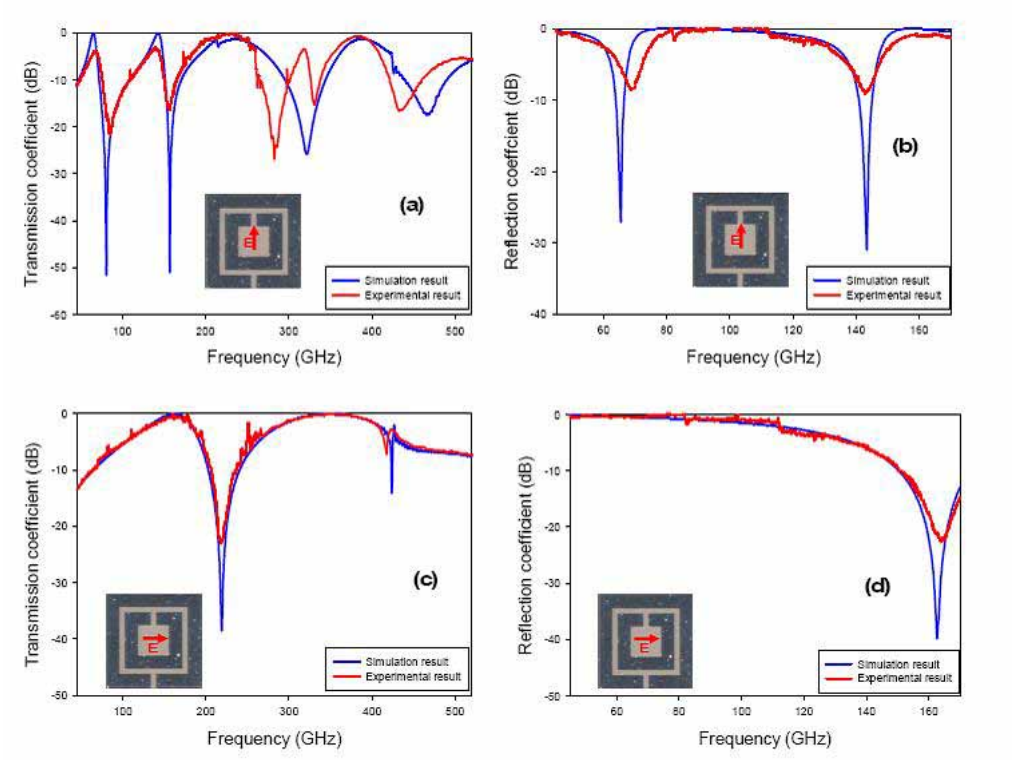

Fig. 3. Simulated (blue) and measured (red) results of fabricated CSRRs array. Co-polar transmission (a) and reflection (b) coefficients. Cross-polar transmission (c) and reflection (d) coefficients.

Conversely, the first co-polar CSRRs resonance dip is placed at 68 GHz. The following upper order resonance is placed at 145 GHz and for the cross-polar case the dip appears at 165 GHz. Also, there is agreement between simulation and experiment.

Looking at the above results one can note one important thing: the criteria for excitation of the higher (non-zero) diffraction harmonics by a periodic structure with the lattice constant g is $\lambda < g\sqrt{\varepsilon}$. So, for g = 0.7mm the 1st non-evanescent diffraction harmonics is exited at $\lambda_{diff,\ air}$ = 0.7mm (f = 429 GHz) for the "air-side" of the structure (it is really seen like an artifact in Figs. 2(a)a and 3(a)). For the "PP-side" of the structure we obtain $\lambda_{diff,\ PP}$ = 0.7mm*1.5 = 1.05mm (f = 286 GHz). It explains existence of the drop in the vicinity of 300GHz (and the appearance of the sixth maximum). This is a Wood's anomaly phenomenon, which in general strongly depends on incident polarization (it explains the difference for co-polar and cross-polar cases), and moreover can differ for structures with different topology. The actual

#100467 - $15.00 USD Received 22 Aug 2008; revised 8 Oct 2008; accepted 10 Oct 2008; published 23 Oct 2008

frequency shift with respect to 286 GHz can be explained by non-normal incidence (strictly, +1 and -1 diffraction harmonics will be excited at different frequencies if $\theta \neq 0$; In the real experiment the incidence angle θ was $\neq 0$ to suppress standing waves in the quasi-optical transmission line, and we estimate it as $\theta \sim 1.5 - 2^0$).

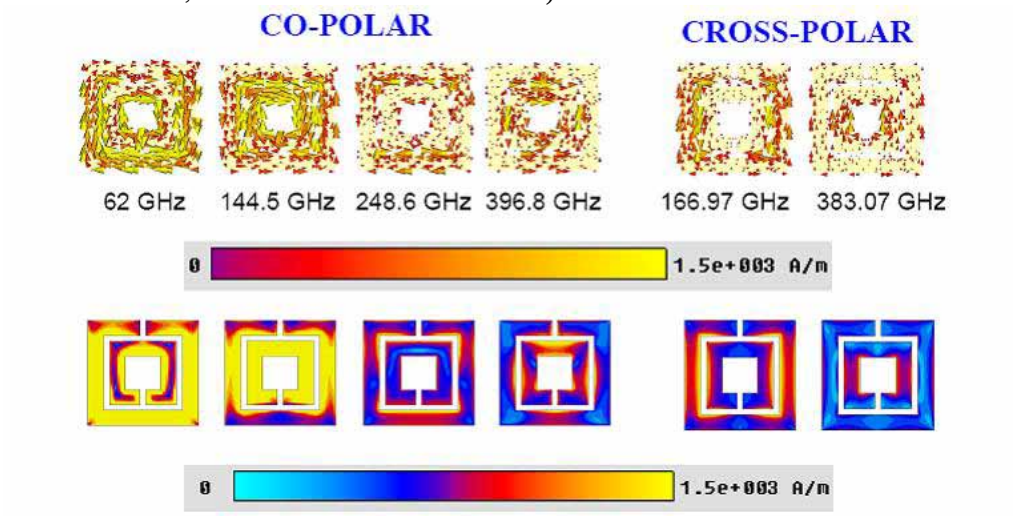

Fig. 4. Simulated surface currents at SRR resonances for co-polar and cross-polar excitations.

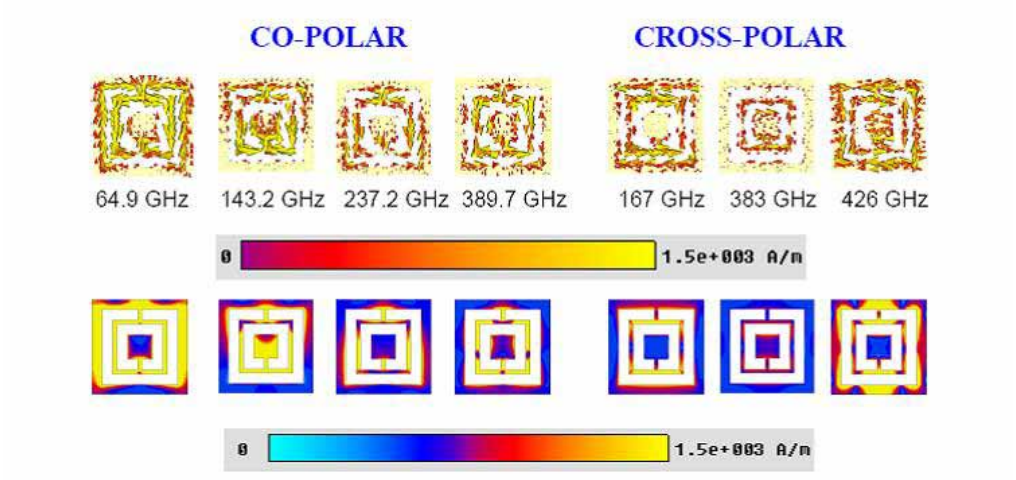

Fig. 5. Simulated surface currents at CSRR resonances for co- and cross-polar excitations.

Moreover, the effects of fabrication tolerances are negligible for the first resonance, and they are evidenced only for some higher order resonances. Their impact in prototypes exhibiting their first resonances in the terahertz range will be analyzed in a future work together with the degradation of frequency response of Al-conductivity.

We have checked the accuracy of the fabrication technology comparing with the analytical model of Refs. 2 and 7: the quasistatic resonance frequencies are 66.4 GHz and 67.7 GHz for SRR and CSRR respectively whereas the experimental values are 67.0 GHz and 68.3 GHz. On the other hand the CST Microwave Studio simulation predicts 62.3 GHz and 65.0 GHz which are in slight disagreement with the previous values, probably due to the finite precision of the simulator.

It is important to notice that the size to wavelength ratios for the SRRs (CSRRs) particles for the co-polar resonances are 0.12λ, 0.26λ, 0.43λ, 0.58λ, and 0.71λ, and for the cross-polar

#100467 - $15.00 USD Received 22 Aug 2008; revised 8 Oct 2008; accepted 10 Oct 2008; published 23 Oct 2008

case we have 0.30λ, and 0.65λ. This implies that except for the first quasistatic resonance the SRRs (CSRRs) particles are no longer in the effective medium limit [2,7] because the size of the SRRs (CSRRs) is much longer than 0.10λ.

Next, we show the simulated surface currents of SRR/CSRR metasurfaces at each dip/peak, to demonstrate the quasi-static or dynamic nature of resonances, see Figs. 4 and 5. The first co-polar resonance shows an almost constant current distribution along the particle, whereas the remaining resonances have marked maxima and minima.

The nature of these resonances will not be the topic of this technological paper, however, a detailed discussion on this topic can be found in [2,16].

5. Conclusions

In this paper we have presented the fabrication of low-loss millimeter wave metamaterials based on patterning on polypropylene substrates operating at millimeter waves. Following the conventional technique of contact photolithography based on industrial equipment we have fabricated two metasurfaces of SRR and CSRR particles by micro-patterning the Al-layer deposited on a supporting polypropilene film substrate with very low loss.

By using numerical simulation tools we have designed the metasurfaces and, then, we have studied numerically and experimentally the transmission properties up to submillimeter wave frequencies (0.5 THz). We have identified both in simulation and experiment several resonances that appear for both co-polar and cross-polar excitations. The agreement is good in almost all realizations, but one of the resonances observed in the co-polar excitation is not predicted by our simulations both in SRRs and CSRRs but a consistent explanation based upon Wood anomalies has been provided. Moreover, the simulated surface currents show that the first co-polar resonance is quasi-static and the rest are dynamic.

These results open the way for the design and construction of fine tuned metamaterials, frequency selective surfaces and spatial filters at millimeter, terahertz and even optical wavelengths.

Acknowledgments

This work was supported by Spanish Government and E.U. FEDER under contracts TEC2005-06923-C03-01 and UPN-00–33–008. Also, Mariem Aznabet and Otman El Mrabet thank AECI support for their grants. The authors are in debt with A. Cortiella and G. Argandoña from CEMITEC for the microscope pictures.

#100467 - $15.00 USD Received 22 Aug 2008; revised 8 Oct 2008; accepted 10 Oct 2008; published 23 Oct 2008